Articles

Relationship of Potency and Resilience to Drug Resistant Mutations for GW420867X Revealed by Crystal Structures of Inhibitor Complexes for Wild-Type, Leu100Ile, Lys101Glu, and Tyr188Cys Mutant HIV-1 Reverse Transcriptases†

Jingshan Ren,‡ Charles E. Nichols,‡ Philip P. Chamberlain,‡ Kurt L. Weaver,§ Steven A. Short,§ Joseph H. Chan,§ Jörg-Peter Kleim,|| and David K. Stammers*,‡

Division of Structural Biology, The Wellcome Trust Centre for Human Genetics, Henry Wellcome Building for Genomic Medicine, University of Oxford, Roosevelt Drive, Oxford, OX3 7BN, United Kingdom, GlaxoSmithKline, Inc., 5 Moore Drive, Research Triangle Park, North Carolina 27709, and GlaxoSmithKline, Medicines Research Centre, Stevenage, Herts, SG1 2NY, United Kingdom

Received September 26, 2006

The selection of drug resistant viruses is a major problem in efforts to combat HIV and AIDS, hence, new compounds are required. We report crystal structures of wild-type and mutant HIV-1 RT with bound non-nucleoside (NNRTI) GW420867X, aimed at investigating the basis for its high potency and improved drug resistance profile compared to the first-generation drug nevirapine. GW420867X occupies a smaller volume than many NNRTIs, yet accesses key regions of the binding pocket. GW420867X has few contacts with Tyr188, hence, explaining the small effect of mutating this residue on inhibitor-binding potency. In a mutated NNRTI pocket, GW420867X either remains in a similar position compared to wild-type (RT(Leu100Ile) and RT(Tyr188Cys)) or rearranges within the pocket (RT(Lys101Glu)). For RT(Leu100Ile), GW420867X does not shift position, in spite of forming different side-chain contacts. The small bulk of GW420867X allows adaptation to a mutated NNRTI binding site by repositioning or readjustment of side-chain contacts with only small reductions in binding affinity.

Introduction

Reverse transcriptase forms a key part of the replicative machinery of retroviruses and has thus been an important target for the development of drugs used in the treatment of HIV infection and AIDS.[1] RT is a multifunctional enzyme that, in addition to DNA polymerase functions, also has RNaseH activity and the ability to bind t-RNA^{lys3}, which is utilized as a primer.[2] HIV-1 RT is expressed in the virus as part of the gag-pol fusion protein and, following cleavage by HIV protease, is found in the virion as a p66/p51 heterodimer.[3] The p66 subunit contains both polymerase and RNaseH active sites and is also able to bind two distinctive classes of drugs.[4−7] First, nucleoside analogue inhibitors (NRTIs) such as zidovudine or lamivudine, which compete (as triphosphates) with nucleotide substrates at the polymerase active site and, following incorporation into the primer strand, cause DNA chain termination.[8] Second, non-nucleoside inhibitors (NNRTIs) bind at an allosteric site distal to the polymerase active site,[4,6] causing inhibition by distortion of three aspartic acid residues that are key for catalysis.[9] NNRTIs are generally specific for HIV-1 RT, although some examples of NNRTI inhibition of HIV-2 RT have been reported, including certain members of the PETT series.[10] The NNRTI binding site shows less amino acid sequence conservation than does the polymerase active site and, thus, can more readily accommodate mutations with less compromise of normal enzymatic function. As a consequence, there is rapid selection of resistant viruses under drug pressure from NNRTIs, precluding the therapeutic use of this class of inhibitor as monotherapy.[11] Nevertheless, NNRTIs have found an important role in treating HIV infection as part of multidrug regimens, which can include NRTIs as well as protease inhibitors.[12] Currently, there are three NNRTIs that are approved for clinical use: nevirapine, delavirdine, and efavirenz. Although the introduction of combination therapy has led to a very significant decline in deaths from AIDS in Western countries, there is now increasing emergence of drug resistant HIV. It is thus important that further new drugs are developed that have limited cross resistance to current mutant forms of the virus. First generation NNRTIs such as nevirapine (Scheme 1) typically lose significant binding affinity even from the effects of single point mutations.[13] Second generation compounds such as efavirenz (Scheme 1) generally have a wider resilience to a range of drug resistance mutations.[14] Further examples of second generation NNRTIs include capravirine (S-1153),[15] etravirine (TMC-125),[16] and quinoxalines such as *S*-3-ethyl-7-fluoro-4-isopropoxy-carbonyl-3,4-dihydro-quinoxalin-2(1*H*)-one (GW420867X[a],[17] Scheme 1), which has progressed into clinical trials.[18,19] We have previously determined crystal structures of a range of NNRTIs in complexes with particular drug resistant HIV-1 RTs,[20−23] while in this report we take a more orthogonal approach. We have thus determined structures of a range of mutant forms of HIV-1 RT (Leu100Ile, Lys101Glu, or Tyr188Cys) in complexes with the same inhibitor, GW420867X, a second generation NNRTI that retains significant activity

† PDB codes for RT−GW420867X complexes: WT, 2opp; L100I, 2opq; K101E, 2opr; Y188C, 2ops.

* To whom correspondence should be addressed. Tel.: +44-1865-287-565. Fax: +44-1865-287-547. E-mail: daves@strubi.ox.ac.uk.

‡ University of Oxford.

§ GlaxoSmithKline, Inc., Research Triangle Park, NC.

|| GlaxoSmithKline, United Kingdom.

[a] Abbreviations: GW420867X, *S*-3-ethyl-7-fluoro-4-isopropoxy- carbonyl-3,4-dihydro-quinoxalin-2(1*H*)-one; HBY097, (*S*)-4-isopropoxycarbonyl-7-methoxy-3-(methylthiomethyl)-3, 4-dihydroquinoxaline-2(1*H*)-thione.

10.1021/jm061117m CCC: $37.00
Published on Web 04/19/2007

Scheme 1

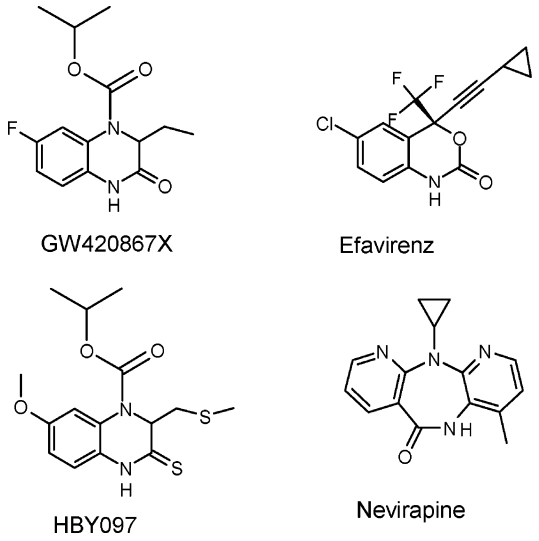

Table 1. Comparison of the Effects of HIV-1 RT Mutations on the Potency of GW420867X, Nevirapine, and Efavirenz[a]

	fold resistance in HIV assay		
	GW420867X	nevirapine	efavirenz
RT(Leu100Ile)	1.4 ± 0.6	7.8 ± 2.3	14.0 ± 9.4
RT(Lys101Glu)	2.5 ± 0.7	13.3 ± 2.4	4.3 ± 0.9
RT(Tyr188Cys)	2.4	25.7 ± 1.4	1.6 ± 0.4

[a] Data from references 17 and 38−44.

against these mutations (Table 1). Such work is aimed at further understanding drug resistance mechanisms at the molecular level and will be of use in the design of novel inhibitors required in continuing efforts to treat HIV infection and AIDS.

Results

Here we report crystal structures of wild-type HIV-1 RT, RT(Leu100Ile), RT(Lys101Glu), and RT(Tyr188Cys) mutants all in complexes with GW420867X, at resolutions ranging from 2.9 Å to 2.3 Å. The structures have been refined with reasonable R-factors while retaining good stereochemistry, as shown in Table 2. The position and conformation of the inhibitor and the mutated residues in each of the complexes are clearly defined in omit difference electron density maps (Figure 1). The average temperature factor for the inhibitor and the amino acid residues immediately surrounding it is much lower compared with that of the rest of the protein, suggesting that the inhibitor is bound with full occupancy and that the NNRTI site is well ordered in each of the structures. As is the case with all published RT structures, a few flexible loops on the protein surface do not have clear electron density and are omitted from the model.

The Structure of the Wild-Type RT−GW420867X. The position and orientation of GW420876X bound in the NNRTI pocket of wild-type RT is shown in Figure 1e. The NNRTI pocket is located between a pair of three-stranded β-sheets (β4, β7−β8, and β9−β11) in the p66 palm domain about 10 Å from the polymerase active site. GW420876X is bound in the NNRTI pocket with its isopropoxy-carbonyl group positioned in the top sub-pocket surrounded by the side chains of Pro95, Tyr181, Tyr188, and Trp229. The quinoxaline ring is sandwiched between the side chains of Leu100 and Val106, while also making edge-on contacts with Val179, Phe227, and Tyr318. The ethyl group occupies the volume essential for triggering the conformational switch of Tyr181.[24] The key hydrogen-bonding interaction from inhibitor to the main-chain of residue Lys101, via the carbonyl group, as seen in many potent NNRTIs when bound to RT, is also present in the RT−GW420867X complex. There is some indication from the electron density map, although not well defined, that a water molecule bridges the two carbonyl oxygens of the inhibitor and the side chain of residue Glu138(p51). A water molecule in a similar position is clearly defined in the higher resolution structure of the RT-(Tyr188Cys)−GW420867X complex.

Comparison of RT−GW420867X with Complexes Containing Nevirapine, Efavirenz, or HBY097. To investigate if there are any structural differences resulting from the binding of different inhibitors, we overlapped the core region of the NNRTI-binding pocket, consisting of 110 structurally conserved RT residues. Using such an approach compensates for the different crystal forms and relative domain rearrangements for the RT heterodimers used in the comparisons. All CA atoms of the 110 residues between RT−GW420867X and RT−nevirapine can be superimposed with an rms deviation of 0.3 Å. Despite both the chemical and the structural differences between nevirapine and GW420867X, they occupy significant amounts of common volume when bound in the NNRTI pocket. Thus, the isopropoxy-carbonyl group and the benzene ring of GW420867X overlap with the two pyridine rings of nevirapine, while the ethyl and cyclopropyl groups are located at the same position (Figure 2a). In the RT−nevirapine structure, two water molecules hydrogen bond to the inhibitor via the pyridine ring nitrogens. One of these nevirapine-bound waters also bridges between the inhibitor and Glu138 via a third water molecule. In the case of RT−GW420867X, the carbonyl oxygen of the quinoxaline ring takes the place of one water molecule of the RT−nevirapine complex and hydrogen bonds to Glu138(p51) via a water molecule, as mentioned above.

The rms deviation between the CA atoms of the NNRTI-pocket protein core of RT−GW420867X and the RT−efavirenz complexes after superimposition is 0.3 Å, indicating there are only small differences in main-chain positions between the two structures. As shown in Figure 2b, the two inhibitors bind in the NNRTI site in a rather similar orientation and while sharing some features in common in their interactions with the protein, there are also differences. The quinoxaline ring is shifted compared to the benzoxazin-2-one ring, with an average shift in atom position of 0.8 Å, maximum shift of 1.0 Å, and an estimated coordinate error for this region of the protein of 0.3 Å. This ring movement also drags the main-chain of residues 101 and 102 with it. While there are some small variations in the positioning of side chains between the two complexes, no large conformational differences are observed. Comparing the locations of the substituents of the two inhibitor ring systems, the isopropoxy-carbonyl group of GW420867X overlaps with the cyclo-propynyl of efavirenz. Interestingly, the ethyl group of GW420867X occupies a similar position to the trifluromethyl of efavirenz, despite the fact that the two groups are located at different substituent positions on the quinoxaline and benzoxazin-2-one rings of the respective inhibitors (Scheme 1). The difference in the puckering of the quinoxaline and benzoxazin-2-one rings accounts for the overlap of these two substituents observed in the crystal structures.

The crystal structure of the quinoxaline HBY097 in complex with HIV-1 RT has been reported (1bqm,).[25] The structural differences between HBY097 and GW420867X involve a substantially altered pattern of substituents (Scheme 1). The lower resolution of the HBY097 structure (3.1 Å) will impose some limitations on coordinate accuracy, nevertheless we are able identify some potential differences. Superimposing the

Table 2. Statistics for Crystallographic Data Collection and Structure Refinement of RT−GW420867X Complexes

		Data Collection Details		
data set	WT	Leu100Ile	Lys101Glu	Tyr188Cys
data collection site	ESRF ID2	ESRF ID14-EH3	ESRF ID14-EH2	SRS PX14.1
wavelength (Å)	0.990	0.931	0.933	1.244
unit cell dimensions (*a*,*b*, *c* in Å)	138.5, 115.3, 65.9	138.4, 114.9, 64.9	138.0, 109.3, 72.4	138.5, 110.3, 72.7
resolution range (Å)	30.0−2.55	30.0−2.80	30.0−2.90	30.0−2.30
observations	161 423	130 986	78 668	176 065
unique reflections	33 166	25 926	23 963	49 585
completeness (%)	94.5	98.7	96.7	98.6
average $I/\sigma(I)$	18.4	10.7	14.2	17.3
R_{merge}[a]	0.052	0.095	0.051	0.060
		Outer Resolution Shell		
resolution range (Å)	2.64−2.55	2.90−2.80	3.00−2.90	2.38−2.30
unique reflections	3187	2539	2160	4759
completeness (%)	92.5	98.6	89.6	96.5
average $I/\sigma(I)$	2.3	1.1	1.1	2.4
		Refinement Statistics		
resolution range (Å)	30.0−2.55	30.0−2.80	30.0−2.90	30.0−2.30
No. of reflections (working/test)	31 281/1657	24 641/1250	22 778/1160	47 075/2472
R-factor[b] (R_{work}/R_{free})	0.207/0.297	0.210/0.274	0.231/0.302	0.218/0.302
R-factor[b] (all data)	0.194	0.202	0.223	0.208
No. of atoms (protein/inhibitor/water)	7618/20/125	7555/20/24	7714/20/-	7748/20/151
rms bond length deviation (Å)	0.010	0.010	0.011	0.010
rms bond angle deviation (°)	1.56	1.56	1.64	1.60
mean B-factor (Å^2)[c]	65/72/37/54	59/64/38/35	89/96/62	56/62/42/45
rms backbone B-factor deviation (Å^2)	6.4	3.5	5.2	6.5

[a] $R_{merge} = \sum|I - \langle I\rangle|/\sum\langle I\rangle$. [b] R-factor $= \sum|F_o - F_c|/\sum F_o$. [c] Mean B factor for main-chain, side-chain, inhibitor, and water molecules.

protein cores of RT−GW420867X and RT−HBY097 gave an rms deviation of 0.8 Å for 108 CA atoms, and the largest displacements occur at residues 111−118 and also in the Pro236 loop region (Figure 2c). The two inhibitors bind at overall similar positions and orientations in the NNRTI pocket. Apparent differences include the quinoxaline ring of HBY097 being about 0.5 Å higher in the pocket than that of GW420867X due to the larger methyl-thiomethylene group at the Tyr181 trigger position. In addition, the phenyl moiety of the quinoxaline ring of HBY097 is somewhat bent compared to the planar conformation seen for GW420867X. GW420867X does not make any closer contact with Tyr188 than 3.6 Å, while HBY097 makes nine contacts within this distance.

Structure of RT(Leu100Ile)−GW420867X. Figure 3a shows the comparison of the NNRTI sites of the wild-type and RT(Leu100Ile)−GW420867X structures. All 110 CA atoms of the core region of the NNRTI-binding pocket can be overlapped with an rms of 0.3 Å, which is within the systematic error of the structures. The inhibitor is bound in a very similar position and orientation in the two structures. The isopropoxy-carbonyl group has relative rotations around the C11−O2 and O2−C12 bonds (162° and −152° for wild-type, −176° and −145° for the mutant), which do not, however, change the number of interactions with the protein. There is a 0.6 Å displacement of the CA atom of the mutated residue Ile100 relative to the wild-type Leu100. The mutated side chain makes three less contacts (≤3.8 Å) to the ispropoxycarbonyl group, but four more interactions to the quinoxaline ring compared to that of the wild-type RT−GW420867X.

Structure of RT(Lys101Glu)−GW420867X. The NNRTI pocket is connected to bulk solvent by a small channel located between residues Lys101, Vall79, and Glu138(p51). A second channel, which has been suggested to be the entrance for inhibitors,[26] is created between the flexible $\beta10-\beta11$ loop and $\beta4$ strand. Lys101 is located at the entrance of the first solvent channel, interacting with inhibitors mainly via its main-chain atoms. The side chain of Lys101 can in some cases form a salt bridge with Glu138(p51), partially sealing off the channel. Glu138(p51) can make interactions with NNRTIs either directly[10] or via water molecules.[6,24] In the wild-type RT−GW420867X complex, the carboxyl group of Glu138 forms a salt-bridge and bifurcated hydrogen bond with the side chain of Lys101, as well as having interactions with the inhibitor via a water molecule. As also observed for the RT(Leu100Ile) and RT(Tyr188Cys) structures, the electron density is well defined for the mutated residue, Glu101 (Figure 1c). However, the side chain of Glu101 folds away from the channel (Figure 3b) to avoid direct contact with Glu138(p51) as a result of electrostatic repulsion, which results in a greater exposure of the inhibitor to solvent. Comparison of the NNRTI sites of wild-type and Lys101Glu mutant RT−GW420867X structures (Figure 3b) gives an rms deviation for 103 CA atoms out of 110 of 0.55 Å.

The largest structural change occurs at the $\beta10-\beta11$ loop, where Trp229 adopts a different conformation to that observed in wild-type RT−GW420867X. This Trp229 conformation is similar to that seen in the RT(Tyr188Cys)−GW420867X complex and appears to be a result of the different crystal forms. An effect of the Lys101Glu mutation is the large shift in the inhibitor position toward Phe227, with an average displacement of 0.5 Å for the inhibitor atoms. This movement can probably be attributed to the opening up of the solvent channel described above. There is also a rotation of ∼30° for the isopropoxy group, which is accompanied by a 50° change of torsion angle χ_2 in residue Tyr181. Other observed changes in side-chain conformation include those at residues Val179, Phe227, and Tyr318.

Structure of RT(Tyr188Cys)−GW420867X. The side chain of Cys188 has clearly defined electron density and adopts a conformation with a $\chi1$ angle of −171° (Figures 1d and 3c).

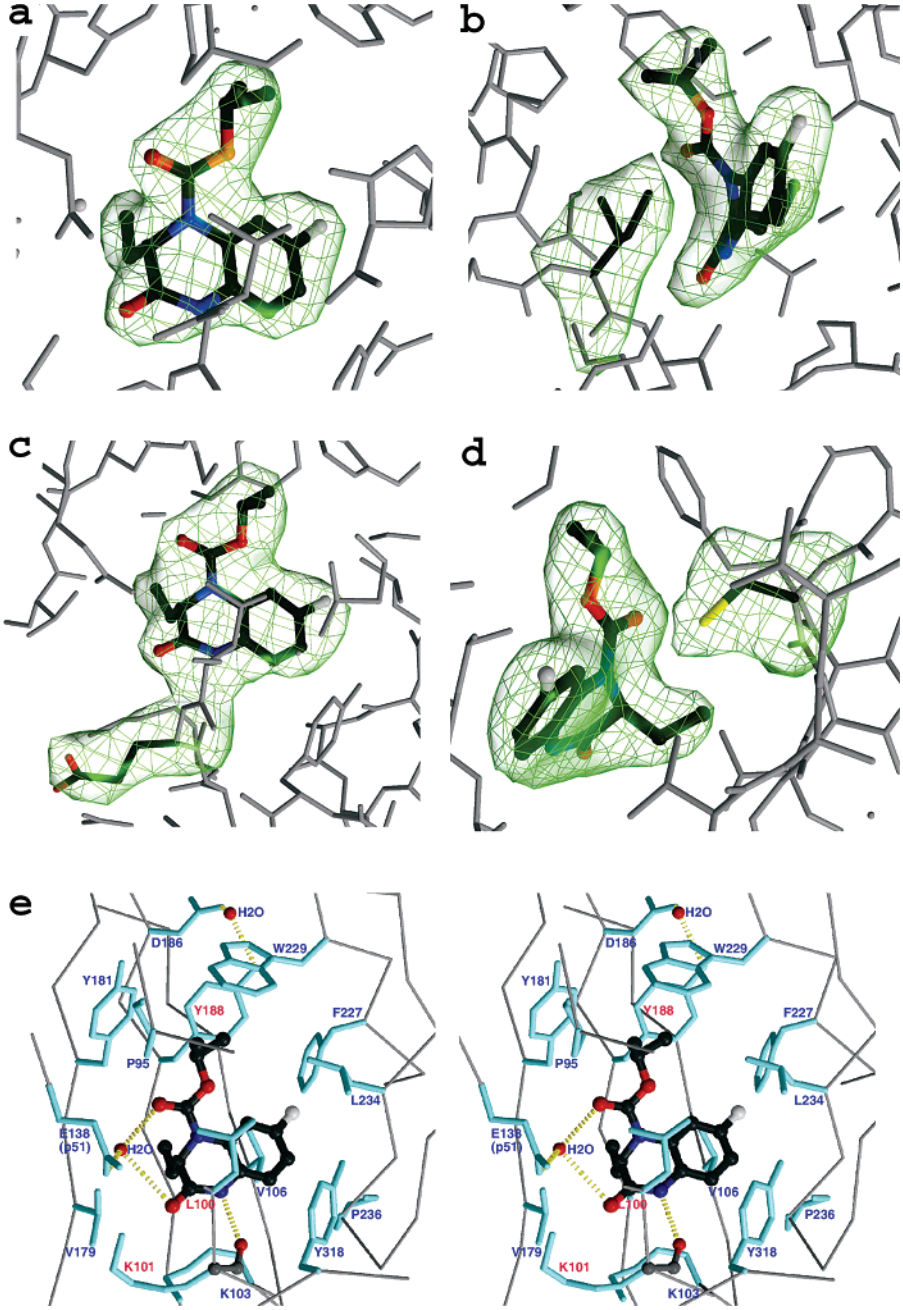

Figure 1. Simulated annealing omit $|f_o| - |f_c|$ maps contoured at 4σ showing electron density for bound GW420867X and, where appropriate, mutated residues at the NNRTI site: (a) wild-type, (b) Leu100Ile, (c) Lys101Glu, and (d) Tyr188Cys RTs. (e) Stereodiagram showing GW420867X bound at the NNRTI site of wild-type RT. The protein CA backbones, side chains, and water molecules are drawn as gray sticks, cyan sticks, and red spheres, respectively. The inhibitor is shown as a ball-and-stick representation and colored by atoms. The broken sticks represent hydrogen bonds. Sites of mutation studied in this report are indicated by side chains labeled in red.

The closest contact between the mutated side chain and the inhibitor is 4.0 Å. When compared with the wild-type RT−GW420867X complex, the inhibitor bound to the mutant RT-(Tyr188Cys) has a very small shift (∼0.2 Å) toward Phe227. The largest conformational difference in the protein occurs at the $\beta9-\beta10$ loop, where Trp229 has a double conformation that has also been observed in the structure of RT−MKC-442.[24] Residue Trp229 is currently modeled to the higher occupancy conformation. By examining our structures of RT, either in complexes with different NNRTIs or in the same complex crystallized with different unit cell parameters, it is clear that the $\beta10-\beta11$ loop is rather flexible and the conformation of Trp229 is correlated with a particular crystal form. Therefore, we can exclude the possibility that the conformational changes in the 229 loop are caused by the Tyr188Cys mutation itself. Additionally, the effect of the Tyr188Cys mutation on other protein residues that interact with the inhibitor is minimal.

We have previously reported crystal structures of RT-(Tyr188Cys) both as an unliganded form as well as in complexes with nevirapine and UC-781.[6,27] The torsion angles of the Cys188 side chain are −50° and −52° for the two structures (nevirapine and UC781, respectively), with the sulfur atom pointing away from the NNRTI pocket, thereby avoiding a clash with the inhibitors. In the unliganded RT structure, the side chain of Cys188 has a similar conformation to that of RT(Tyr188Cys)-GW420867X.

Discussion

HIV-1 RT−GW420867X Interactions Related to Binding Potency. The internal surface of the NNRTI pocket is mainly

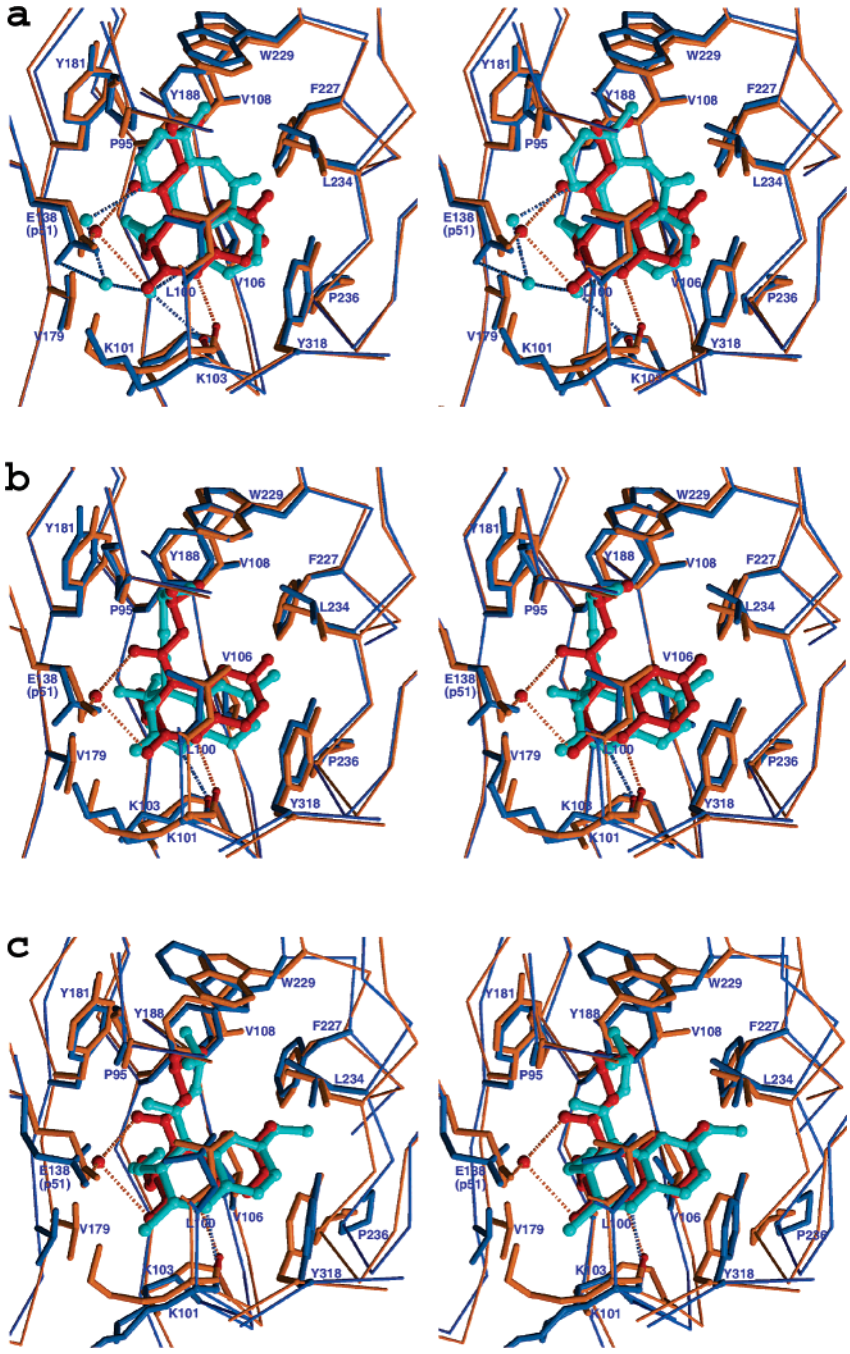

Figure 2. Stereodiagrams comparing the NNRTI site of wild-type RT−GW420867X with (a) RT−nevirapine, (b) RT−efavirenz, and (c) RT−HBY097 complexes. The thinner and thicker bonds show the protein CA backbones and side chains, respectively. RT−GW420867X is colored in orange and the other NNRTIs in blue. The inhibitors and waters are shown as a ball-and-stick representation, with GW420867X colored in red and the others in cyan. The broken lines represent hydrogen bonds between the protein and the inhibitors.

composed of hydrophobic residues with relatively few hydrophilic residues located in the vicinity of the inhibitor. The key residues that interact with inhibitors include Leu100, Lys101, Lys103, Val106, Val179, Tyr181, Tyr188, Phe227, Trp229, and Tyr318. To understand the mode of inhibition by NNRTIs, the structural requirements for a powerful inhibitor, the nature of key protein−inhibitor interactions together with the factors that contribute to resilience to drug-resistance mutations, we have determined a large number of structures of wild-type and drug-resistant mutant RT−NNRTI complexes. The inhibitors we have studied so far include both chemically divergent as well as related analogues from within the same series, yet with widely differing potencies. The NNRTI binding pocket does not exist in the unliganded protein, where the hydrophobic surfaces of the two β-sheets, $\beta4-\beta7-\beta8$ and $\beta9-\beta10-\beta11$, are collapsed on to one another. Upon the binding of inhibitor, the side chains of Tyr181 and Tyr188, contained within the $\beta4-\beta7-\beta8$ sheet, flip conformation from a "down" to an "up" position, thereby leading to the creation of the NNRTI pocket. The change, meanwhile, also distorts the conformation of the polymerase active site whose three catalytic aspartic residues, contained in the $\beta4-\beta7-\beta8$ sheet, thereby leading to inhibition of the enzyme. As we have reported previously, the $\beta9-\beta10-\beta11$ sheet is able to adopt various positions dependent upon the binding of different sized inhibitors, therefore, altering the size of the pocket.[24,26,28,29] On the other hand, the protein side chains lining the pocket are also flexible and can readily adopt different conformations to interact with various groups from

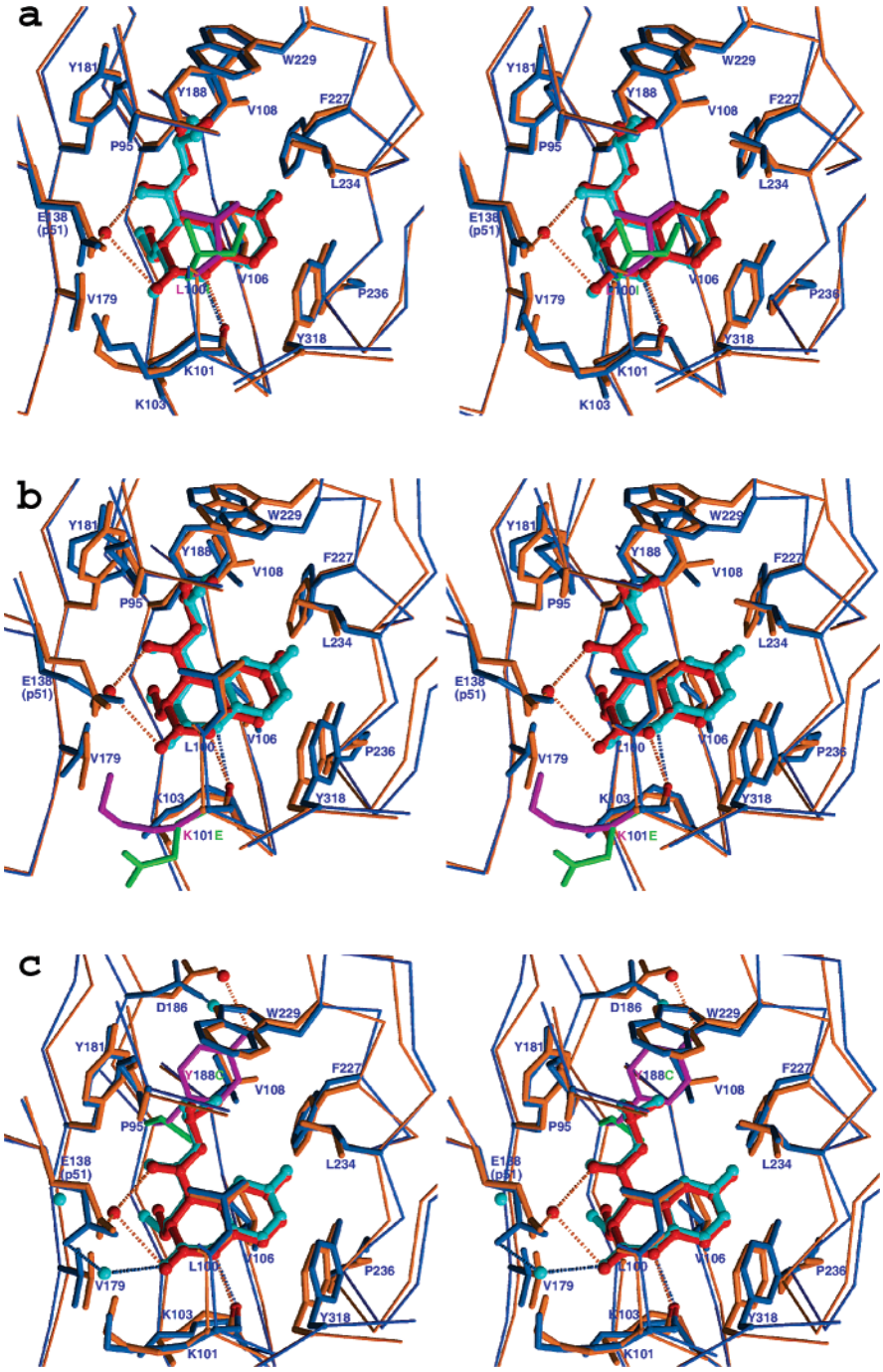

Figure 3. Stereodiagrams comparing the NNRTI site of wild-type RT−GW420867X with (a) RT(Leu100Ile), (b) RT(Lys101Glu), and (c) RT-(Tyr188Cys)−GW420867X complexes. The protein CA backbones and side chains are shown as thinner and thicker bonds, respectively. Wild-type RT is colored as orange and mutant RT as blue. The inhibitor is shown in red for wild-type RT and in cyan for the mutant RTs. For clarity, the side chains of the mutation sites are colored as magenta for wild-type and green for mutant RTs.

chemically divergent inhibitors without significantly altering the overall volume of the binding site. It is perhaps the flexible nature of this region that allows the accommodation of a wide range of mutations that largely are without affect on the architecture of the active site, which is positioned only some 10 Å away.

Most first generation NNRTIs, such as MKC-442 and α-APA, have a two-hinged-ring moiety.[6,27] When bound in the NNRTI pocket, the "upper ring" occupies the top subpocket, making ring-stacking interactions with Tyr181 and Tyr188, as well as additional contacts with Trp229 and Leu234. The "lower ring" is positioned at a region surrounded by the main chains of residues 101−103 and 236 and side chains of Lys103, Val106, Phe227, and Tyr318. In addition, there is always a moiety in the various NNRTIs studied to date that occupies a small volume in the region of Gly190, Val179, and Tyr181. This is referred to as the "Tyr181 triggering position", and examples include the isopropyl group of MKC-442, the cyclopropyl group of nevirapine, and the 5-methyl group of 9-C1-TIBO. The importance of this small volume for NNRTI binding has been shown in the structural and SAR studies of the first generation NNRTIs of the HEPT chemical series.[24,30] HEPT binds in the pocket with the 5-methyl group of the pyrimidine ring occupying the small volume near Val179 with Tyr181 in the unliganded conformation. MKC-442 has a larger isopropyl group at the 5-position and binds to the enzyme 2000-fold tighter than HEPT

and with Tyr181 positioned in the normal inhibitor-bound conformation. Replacement of the 5-methyl of HEPT with a hydrogen atom leads to a complete loss of potency. In the case of GW42087X, positioning of Tyr181 will make a smaller contribution to the binding energy as contacts with the side chain are limited and do not involve aromatic ring stacking. A further key interaction that most potent inhibitors possess is a hydrogen bond to the carbonyl oxygen of Lys101. The volume of the NNRTI pocket varies with the sizes of the bound inhibitor, while the inhibitors themselves have volumes ranging from 230 Å^3 for nevirapine to 365 Å^3 for S-1153. By superimposing representative structures of nine previously reported NNRTIs of different chemical series (excluding BHAP, which extends toward the outer region of the pocket), these inhibitors span a volume of 590 Å,^{3} of which 75 Å^3 is shared in common. GW420867X is a relatively small molecule with a volume of 236 Å^3 and, therefore, unable to make as many interactions with the protein as larger NNRTIs, yet paradoxically is one of the most potent NNRTIs with an EC_{50} against HIV-1 of 1.1 nM. The question arises as to what makes GW420867X a potent inhibitor. The crystal structures of RT−GW420867X enabled us to understand features that contribute to the inhibitor potency as well as its resilience to drug-resistance mutations. From the comparisons of the binding mode of GW420867X with other NNRTIs, it is clear that GW420867X possesses all the key binding features of the second generation NNRTIs, efavirenz and UC-781.[20,31] Thus, the smaller nonaromatic isopropoxy-carbonyl group of GW420867X is positioned in the "top-ring" region of the NNRTI pocket, making interactions with Pro95, Tyr181, Tyr188, and Trp229, corresponding to the cyclopropyl-propynyl group of efavirenz and the dimethylallyl group of UC-781. The quinoxaline ring is positioned at the "lower-ring" part of the pocket, contacting Leu100, Val106, Val179, Phe227, and Tyr318, and making a strong hydrogen bond with the carbonyl oxygen of Lys101, analogous to the benzoxazin-2-one ring of efavirenz[20] and the thiocarboxanilide group of UC-781.[31] Finally, the ethyl group occupies the Tyr181 triggering position, playing a similar role as the trifluoromethyl group of efavirenz and the furanyl ring of UC-781. The spatial overlaps of GW420867X with efavirenz and UC781 are also significant. If RT−GW420867X is included in overlaps with nine other RT−NNRTI structures, it occupies 73 Å^3 out of the 75 Å^3 common volume, while sharing 78 and 83% of the volume with efavirenz and UC-781, respectively.

Structural Features Related to Drug Resistance In cell culture, GW420867X in combination with an NRTI such as lamivudine (3TC) or abacavir (ABC), was selected for a range of NNRTI-specific resistance mutations: Leu100Val, Lys101Glu, Lys103Arg, Val106Ala, Val108Ile, Tyr181Cys, and Tyr188His.[17] However, GW420867X, in common with efavirenz and UC-781, maintained higher levels of activity against mutant virus strains than the first-generation NNRTIs, nevirapine and delavirdine. A number of crystal structures of both wild-type and mutant RT−NNRTI complexes have been reported.[4,6,10,20−25,27−29,32,33] By comparing the wild-type RT−GW420867X, mutant RT−GW420867X complexes, and those in the data base, we may dissect out structural information that could provide explanations for the reported resistance profile of GW420867X.

Leu100Ile. GW420867X shows only a small reduction in potency against the Leu100Ile mutant virus in contrast to an ∼8-fold reduction for nevirapine (Table 1). This retention of the potency of GW420867X could be well explained by the observations from the crystal structures of both wild-type and Leu100Ile mutant RT complexes with these inhibitors. Residue 100 interacts with the central part of most NNRTIs and appears to have a role of positioning the inhibitors in the binding site.[22] A leucine to isoleucine change resulted in significant rearrangement of nevirapine and UC-781 in the binding pocket, which in turn alters protein−inhibitor interactions, especially with Tyr181 and Tyr188.[22] However, we see no significant changes in position and orientation of GW420867X for the Leu100Ile mutant. Although Ile100 interacts with a different part of the inhibitor compared to Leu100, the mutation does not give a pronounced alteration in the total number of protein−inhibitor interactions.

Lys101Glu. RT(Lys101Glu) shows resistance to many NNRTIs, including a low level for GW420867X (2.5-fold) and a moderate level for nevirapine (∼13-fold) (Table 1). Although interactions between the protein and the NNRTIs are predominantly hydrophobic, there are polar interactions that include hydrogen bonds directly to protein atoms as well as indirectly via water molecules. Lys101 is located at the entrance of the small solvent channel leading to the inhibitor site and forms a salt bridge with Glu138(p51). In turn, Glu138(p51) can interact with certain NNRTIs via a network of water molecules, as seen in some higher resolution RT−inhibitor complexes such as nevirapine.[6] A change from positive to negative charge results in the side chain of Glu101 folding away from the NNRTI site and thus removing the neutralizing effect on the negative charge of Glu138(p51). A net negative charge is positioned at the entrance of the small solvent channel leading to the NNRTI site. The mutation of Glu138Lys will produce the opposite effect and place a net positive charge in this region. It is unlikely that such charge changes will have a direct effect on GW420867X binding as the inhibitor, like most NNRTIs, carries no net charge. Nevertheless, changes in the electrostatic environment disturb the local protein conformation and in turn the solvent structure, which may therefore have effects on NNRTI binding in some cases. We have indeed observed conformation changes for mutations at residues 101 and 138 as well as the movements of water molecules, which are accompanied by small shifts of inhibitor position in the higher resolution structures of both Lys101Glu and Glu138Lys mutant RT−nevirapine complexes.[23] The shift in inhibitor position and the disruption of protein−inhibitor interactions in the RT(Lys101Glu)−GW420867X complex, although we have been unable to model the solvent structure due to the lower resolution, are the largest among the three mutant complexes reported here. In spite of such differences, the loss of potency is small, indicating that GW420867X is able to productively rearrange its position within the context of the mutated NNRTI binding pocket in this case.

Tyr188Cys. The Tyr188Cys mutation gives 2.5-fold resistance to GW420867X compared to ∼26-fold resistance to nevirapine (Table 1). We have previously reported the structure of the RT(Tyr188Cys)−nevirapine complex, in which the inhibitor shows a large shift in the binding site compared to RT wild-type, giving significant change in protein−inhibitor contacts.[21] However, the altered interactions are unable to compensate for the loss of ring-stacking interactions of nevirapine with Tyr188, thus giving rise to high-level resistance. There is no significant conformation change in either protein or GW420867X resulting from the Tyr188Cys mutation. Although two van der Waals contacts between the isopropoxy-carbonyl group and the ring of Tyr188 are lost; such interactions are unlikely to be predominant contributors to the binding energy of GW420876X, in contrast to the case with nevirapine, where aromatic stacking of a pyridine ring is significant. Thus, the insensitivity of GW420867X to RT(Tyr188Cys) is explained

by its binding being less dependent on ring-stacking interactions with the tyrosine side chain. Hence, mutation of Tyr188 to a less bulky aliphatic residue has relatively small effects on the tightness of the binding of this inhibitor.

The structural data reported here give insights into the structural basis for the high potency of GW420867X. The overall shape and chemical structure of GW420867X enables the compound to occupy all the key volumes in the NNRTI pocket, and thereby form protein−inhibitor interactions characteristic of second generation NNRTIs, such as UC781 and efavirenz. Additionally the structures of mutant RT complexes indicate how GW420867X can adapt to the altered stereochemistry of the NNRTI site by rearrangement within the pocket or forming different side-chain contacts. The availability of refined coordinate sets of wild-type and mutant RT with bound GW420867X will assist in the design of further NNRTIs. First, different subsituent types and positions can be explored for the quinoxaline ring, and structural data will provide constraints. A broader structure-based design approach can make use of some structural features of GW420867X important for interacting with RT in combination with other NNRTIs whose structures are known to generate novel templates for further optimization. New generation NNRTIs are required as part of an evolving combination therapy approaches to combat drug resistance and enable the continued fight against HIV and AIDS.

Experimental Section

Crystallization, Data Collection, and Structure Determination. Crystals of wild-type and mutant RT−GW420867X complexes were grown at 4 °C using the sitting drop vapor diffusion method, as described previously.[34] The crystals were partially dehydrated by increasing the PEG 3350 concentration from 6% to 50% in stages over 3 days prior to data collection. X-ray data for the RT wild-type, RT(Leu100Ile), and RT(Lys101Glu) mutants were collected at ESRF, Grenoble, France. The data collection for the mutant RT-(Tyr188Cys)−GW420867X complex was carried out at SRS, Daresbury, U.K. Crystals were flash frozen in liquid propane, transferred into a cooled nitrogen stream, and maintained at 100 K during data collection. Data were collected as frames of 1° oscillations, which were indexed and integrated using DENZO; subsequent data merging was carried out with SCALEPACK.[35] The orientations and positions of RT molecules in the unit cells of the four RT complexes crystals were determined with rigid-body refinement using initial models of RT−efavirenz (1fk9),[20] for the wild-type and Leu100Ile mutant, and RT−MKC-442 (1rt1),[24] for the RT(Lys101Glu) and RT(Tyr188Cys) mutants. The difference electron density maps clearly showed the GW420867X bound in the NNRTI pocket together with the mutated side chains, allowing the inhibitor to be modeled without difficulty in each case. All the structures were then refined with CNS[36] using positional, simulated annealing, and individual B-factor refinement with anisotropic B-factor scaling and bulk solvent correction. The parameters for GW420867X used in the refinement were generated from the small molecule crystal structure provided by Dr. E. F. Paulus, Hoechst-Bayer, Germany. Model rebuilding was carried out with O.[37] For data sets with a lower reflections-to-parameters ratio, that is, RT(Leu100Ile) and RT(Lys101Glu), tight positional restraints were applied to atoms distal to the NNRTI site (defined as >20 Å from the CA of Tyr188) during refinement. The X-ray data collection and crystallographic refinement statistics are shown in Table 2.

Acknowledgment. We thank the staff at the following synchrotrons for their assistance in data collection: the ESRF, Grenoble, France, and the SRS, Daresbury, United Kingdom. Supporting grants from the Medical Research Council and the EU (QLKT-2000-00291, QLKT2-CT-2002-01311) to D.K.S. are acknowledged.

References

(1) De Clercq, E. New developments in anti-HIV chemotherapy. *Curr. Med. Chem.* **2001**, *8* (13), 1543−1572.
(2) Goff, S. P. Retroviral reverse transcriptase: Synthesis, structure, and function. *J. Acquired Immune Defic. Syndr.* **1990**, *3*, 817−831.
(3) Di Marzo Veronese, F.; Copeland, T. D.; De Vico, A. L.; Rahman, R.; Oroszlan, S.; Gallo, R. C.; Sarngadharan, M. G. Characterization of highly immunogenic p66/p51 as the reverse transcriptase of HTLV-III/LAV. *Science* **1986**, *231*, 1289−1291.
(4) Kohlstaedt, L. A.; Wang, J.; Friedman, J. M.; Rice, P. A.; Steitz, T. A. Crystal structure at 3.5 Å resolution of HIV-1 reverse transcriptase complexed with an inhibitor. *Science* **1992**, *256*, 1783−1790.
(5) Jacobo-Molina, A.; Ding, J. P.; Nanni, R. G.; Clark, A. D. J.; Lu, X.; Tantillo, C.; Williams, R. L.; Kamer, G.; Ferris, A. L.; Clark, P.; Hizi, A.; Hughes, S. H.; Arnold, E. Crystal structure of human immunodeficiency virus type 1 reverse transcriptase complexed with double-stranded DNA at 3.0 Å resolution shows bent DNA. *Proc. Natl. Acad. Sci. U.S.A.* **1993**, *90*, 6320−6324.
(6) Ren, J.; Esnouf, R.; Garman, E.; Somers, D.; Ross, C.; Kirby, I.; Keeling, J.; Darby, G.; Jones, Y.; Stuart, D.; Stammers, D. High resolution structures of HIV-1 RT from four RT−inhibitor complexes. *Nature Structural Biology* **1995**, *2*, 293−302.
(7) Rodgers, D. W.; Gamblin, S. J.; Harris, B. A.; Ray, S.; Culp, J. S.; Hellmig, B.; Woolf, D. J.; Debouck, C.; Harrison, S. C. The structure of unliganded reverse transcriptase from the human immunodeficiency virus type 1. *Proc. Natl. Acad. Sci. U.S.A.* **1995**, *92*, 1222−1226.
(8) Huang, H.; Chopra, R.; Verdine, G. L.; Harrison, S. C. Structure of a covalently trapped catalytic complex of HIV-1 reverse transcriptase: Implications for drug resistance. *Science* **1998**, *282*, 1669−1675.
(9) Esnouf, R.; Ren, J.; Ross, C.; Jones, Y.; Stammers, D.; Stuart, D. Mechanism of inhibition of HIV-1 reverse transcriptase by non-nucleoside inhibitors. *Nat. Struct. Biol.* **1995**, *2*, 303−308.
(10) Ren, J.; Diprose, J.; Warren, J.; Esnouf, R. M.; Bird, L. E.; Ikemizu, S.; Slater, M.; Milton, J.; Balzarini, J.; Stuart, D. I.; Stammers, D. K. Phenylethylthiazolylthiourea (PETT) non-nucleoside inhibitors of HIV-1 and HIV-2 reverse transcriptases: Structural and biochemical analyses. *J. Biol. Chem.* **2000**, *275*, 5633−5639.
(11) Richman, D.; Shih, C.-K.; Lowy, I.; Rose, J.; Prodanovich, P.; Goff, S.; Griffin, J. Human immunodeficiency virus type 1 mutants resistant to non-nucleoside inhibitors of reverse transcriptase arise in tissue culture. *Proc. Natl. Acad. Sci. U.S.A.* **1991**, *88*, 11241−11245.
(12) Moyle, G. The emerging roles of non-nucleoside reverse transcriptase inhibitors in antiretroviral therapy. *Drugs* **2001**, *61*, 19−26.
(13) Sardana, V. V.; Emini, E. A.; Gotlib, L.; Graham, D. J.; Lineberger, D. W.; Long, W. J.; Wolfgang, J. A.; Condra, J. H. Functional analysis of HIV-1 reverse transcriptase amino acids involved in resistance to multiple nonnucleoside inhibitors. *J. Biol. Chem.* **1992**, *267*, 17526−17530.
(14) Young, S. D.; Britcher, S. F.; Tran, L. O.; Payne, L. S.; Lumma, W. C.; Lyle, T. A.; Huff, J. R.; Anderson, P. S.; Olsen, D. B.; Carroll, S. S.; Pettibone, D. J.; O'Brien, J. A.; Ball, R. G.; Balani, S. K.; Lin, J. H.; Chen, I.-W.; Schleif, W. A.; Sardana, V. V.; Long, W. J.; Byrnes, V. W.; Emini, E. A. L-743,726 (DMP-266): A novel, highly potent nonnucleoside inhibitor of the human immunodeficiency virus type 1 reverse transcriptase. *Antimicrob. Agents Chemother.* **1995**, *39*, 2602−2605.
(15) Fujiwara, T.; Sato, A.; el-Farrash, M.; Miki, S.; Abe, K.; Isaka, Y.; Kodama, M.; Wu, Y.; Chen, L. B.; Harada, H.; Sugimoto, H.; Hatanaka, M.; Hinuma, Y. S-1153 inhibits replication of known drug-resistant strains of human immunodeficiency virus type 1. *Antimicrob. Agents Chemother.* **1998**, *42*, 1340−1345.
(16) Das, K.; Clark, A. D., Jr.; Lewi, P. J.; Heeres, J.; De Jonge, M. R.; Koymans, L. M.; Vinkers, H. M.; Daeyaert, F.; Ludovici, D. W.; Kukla, M. J.; De Corte, B.; Kavash, R. W.; Ho, C. Y.; Ye, H.; Lichtenstein, M. A.; Andries, K.; Pauwels, R.; De Bethune, M. P.; Boyer, P. L.; Clark, P.; Hughes, S. H.; Janssen, P. A.; Arnold, E. Roles of conformational and positional adaptability in structure-based design of TMC125−R165335 (etravirine) and related non-nucleoside reverse transcriptase inhibitors that are highly potent and effective against wild-type and drug-resistant HIV-1 variants. *J. Med. Chem.* **2004**, *47*, 2550−2560.
(17) Balzarini, J.; De Clercq, E.; Carbonez, A.; Burt, V.; Kleim, J. P. Long-term exposure of HIV type 1-infected cell cultures to combinations of the novel quinoxaline GW420867X with lamivudine, abacavir, and a variety of nonnucleoside reverse transcriptase inhibitors. *AIDS Res. Hum. Retroviruses* **2000**, *16*, 517−528.

(18) Arasteh, K.; Wood, R.; Muller, M.; Prince, W.; Cass, L.; Moore, K. H.; Dallow, N.; Jones, A.; Klein, A.; Burt, V.; Kleim, J. P. GW420867X administered to HIV-1-infected patients alone and in combination with lamivudine and zidovudine. *HIV Clin. Trials* **2001**, *2* (4), 307−16.
(19) Moore, K. H.; Cass, L. M.; Dallow, N.; Hardman, T. C.; Jones, A.; Boyce, M.; Prince, W. T. Pharmacokinetics and tolerability of GW420867X, a nonnucleoside reverse transcriptase inhibitor, following single escalating doses in healthy male volunteers. *J. Clin. Pharmacol.* **2001**, *41* (10), 1098−105.
(20) Ren, J.; Milton, J.; Weaver, K. L.; Short, S. A.; Stuart, D. I.; Stammers, D. K. Structural basis for the resilience of efavirenz (DMP-266) to drug resistance mutations in HIV-1 reverse transcriptase. *Struct. Fold. Des.* **2000**, *8*, 1089−1094.
(21) Ren, J.; Nichols, C.; Bird, L.; Chamberlain, P.; Weaver, K.; Short, S.; Stuart, D. I.; Stammers, D. K. Structural mechanisms of drug resistance for mutations at codons 181 and 188 in HIV-1 reverse transcriptase and the improved resilience of second generation non-nucleoside inhibitors. *J. Mol. Biol.* **2001**, *312* (4), 795−805.
(22) Ren, J.; Nichols, C. E.; Chamberlain, P. P.; Weaver, K. L.; Short, S. A.; Stammers, D. K. Crystal structures of HIV-1 reverse transcriptase mutated at codons 100, 106 and 108 and mechanisms of resistance to non-nucleoside inhibitors. *J. Mol. Biol.* **2004**, *336*, 569−578.
(23) Ren, J.; Nichols, C. E.; Stamp, A.; Chamberlain, P. P.; Ferris, R.; Weaver, K. L.; Short, S. A.; Stammers, D. K. Structural insights into mechanisms of non-nucleoside drug resistance for HIV-1 reverse transcriptases mutated at codons 101 or 138. *FEBS J.* **2006**, *273* (16), 3850−3860.
(24) Hopkins, A. L.; Ren, J.; Esnouf, R. M.; Willcox, B. E.; Jones, E. Y.; Ross, C.; Miyasaka, T.; Walker, R. T.; Tanaka, H.; Stammers, D. K.; Stuart, D. I. Complexes of HIV-1 reverse transcriptase with inhibitors of the HEPT series reveal conformational changes relevant to the design of potent non-nucleoside inhibitors. *J. Med. Chem.* **1996**, *39*, 1589−1600.
(25) Hsiou, Y.; Das, K.; Ding, J.; Clark, A. D.; Kleim, J.-P.; Rosner, M.; Winkler, I.; Riess, G.; Hughes, S. H.; Arnold, E. HIV-1 reverse transcriptase complexed with the non-nucleoside inhibitor HBY 097: Inhibitor flexibility is a useful design feature for reducing drug resistance. *J. Mol. Biol.* **1998**, *284*, 313−323.
(26) Esnouf, R. M.; Ren, J.; Hopkins, A. L.; Ross, C. K.; Jones, E. Y.; Stammers, D. K.; Stuart, D. I. Unique features in the structure of the complex between HIV-1 reverse transcriptase and the bis(heteroaryl)-piperazine (BHAP) U-90152 explain resistance mutations for this non-nucleoside inhibitor. *Proc. Natl. Acad. Sci. U.S.A.* **1997**, *94*, 3984−3989.
(27) Ding, J.; Das, K.; Moereels, H.; Koymans, L.; Andries, K.; Janssen, P. A. J.; Hughes, S. H.; Arnold, E. Structure of HIV-1 RT/TIBO R 86183 complex reveals similarity in the binding of diverse non-nucleoside inhibitors. *Nat. Struct. Biol.* **1995**, *2*, 407−415.
(28) Ren, J.; Esnouf, R.; Hopkins, A.; Ross, C.; Jones, Y.; Stammers, D.; Stuart, D. The structure of HIV-1 reverse transcriptase complexed with 9-chloro-TIBO: Lessons for inhibitor design. *Structure* **1995**, *3*, 915−926.
(29) Ren, J.; Nichols, C. E.; Bird, L. E.; Fujiwara, T.; Sugimoto, H.; Stuart, D. I.; Stammers, D. K. Binding of the second generation non-nucleoside inhibitor S-1153 to HIV-1 RT involves extensive main chain hydrogen bonding. *J. Biol. Chem.* **2000**, *275*, 14316−14320.
(30) Tanaka, H.; Baba, M.; Hayakawa, H.; Sakamaki, T.; Miyasaka, T.; Ubasawa, M.; Takashima, H.; Sekiya, K.; Nitta, I.; Shigeta, S.; Walker, R. T.; Balzarini, J.; De Clercq, E. A new class of HIV-1-specific 6-substituted acyclouridine derivatives: synthesis and anti-HIV-1 activity of 5- or 6- substituted analogues of 1-[(2-hydroxyethoxy)methyl]-6-(phenylthio)thymine (HEPT). *J. Med. Chem.* **1991**, *34*, 349−357.
(31) Ren, J.; Esnouf, R. M.; Hopkins, A. L.; Warren, J.; Balzarini, J.; Stuart, D. I.; Stammers, D. K. Crystal structures of HIV-1 reverse transcriptase in complex with carboxanilide derivatives. *Biochemistry* **1998**, *37*, 14394−14403.
(32) Ding, J.; Das, K.; Tantillo, C.; Zhang, W.; Clark, A. D. J.; Jessen, S.; Lu, X.; Hsiou, Y.; Jacobo-Molina, A.; Andries, K.; Pauwels, R.; Moereels, H.; Koymans, L.; Janssen, P. A. J.; Smith, R. H. J.; Kroeger Koepke, R.; Michejda, C. J.; Hughes, S. H.; Arnold, E. Structure of HIV-1 reverse transcriptase in a complex with the non-nucleoside inhibitor α-APA R 95845 at 2.8 Å resolution. *Structure* **1995**, *3*, 365−379.
(33) Das, K.; Ding, J.; Hsiou, Y.; Clark, A. D.; Moereels, H.; Koymans, L.; Andries, K.; Pauwels, R.; Janssen, P. A.; Boyer, P. L.; Clark, P.; Smith, R. H.; Kroeger Smith, M. B.; Michejda, C. J.; Hughes, S. H.; Arnold, E. Crystal structures of 8-Cl and 9-Cl TIBO complexed with wild-type HIV-1 RT and 8-Cl TIBO complexed with the Tyr181Cys HIV-1 RT drug-resistant mutant. *J. Mol. Biol.* **1996**, *264*, 1085−1100.
(34) Stammers, D. K.; Somers, D. O. N.; Ross, C. K.; Kirby, I.; Ray, P. H.; Wilson, J. E.; Norman, M.; Ren, J. S.; Esnouf, R. M.; Garman, E. F.; Jones, E. Y.; Stuart, D. I. Crystals of HIV-1 reverse transcriptase diffracting to 2.2Å resolution. *J. Mol. Biol.* **1994**, *242*, 586−588.
(35) Otwinowski, Z.; Minor, W. Processing of X-ray diffraction data collected in oscillation mode. *Methods Enzymol.* **1996**, *276*, 307−326.
(36) Brunger, A. T.; Adams, P. D.; Clore, G. M.; Delano, W. L.; Gros, P.; Grosse, K. R. W.; Jiang, J. S.; Kuszewski, J.; Nilges, M.; Pannu, N. S.; Read, R. J.; Rice, L. M.; Simonson, T.; Warren, G. L. Crystallography and NMR system: A new software suite for macromolecular structure determination. *Acta Crystallogr.* **1998**, *D54*, 905−921.
(37) Jones, T. A.; Zou, J. Y.; Cowan, S. W.; Kjeldgaard, M. Improved methods for building protein models in electron density maps and the location of errors in these models. *Acta Crystallogr.* **1991**, *A47*, 110−119.
(38) Balzarini, J.; Pelemans, H.; Aquaro, S.; Perno, C. F.; Witvrouw, M.; Schols, D.; De Clercq, E.; Karlsson, A. Highly favorable antiviral activity and resistance profile of the novel thiocarboxanilide pentenyloxy ether derivatives UC-781 and UC-82 as inhibitors of human immunodeficiency virus type 1 replication. *Mol. Pharmacol.* **1996**, *50*, 394−401.
(39) Buckheit, R. W.; Snow, M. J.; Fliakas-Boltz, V.; Kinjerski, T. L.; Russell, J. D.; Pallansch, L. A.; Brouwer, W. G.; Yang, S. S. Highly potent oxathiin carboxanilide derivatives with efficacy against nonnucleoside reverse transcriptase inhibitor-resistant human immunodeficiency virus isolates. *Antimicrob. Agents Chemother.* **1997**, *41*, 831−837.
(40) Chan, J. H.; Hong, J. S.; Hunter, R. N., III; Orr, G. F.; Cowan, J. R.; Sherman, D. B.; Sparks, S. M.; Reitter, B. E.; Andrews, C. W., III; Hazen, R. J.; St Clair, M.; Boone, L. R.; Ferris, R. G.; Creech, K. L.; Roberts, G. B.; Short, S. A.; Weaver, K.; Ott, R. J.; Ren, J.; Hopkins, A.; Stuart, D. I.; Stammers, D. K. 2-Amino-6-arylsulfonylbenzonitriles as non-nucleoside reverse transcriptase inhibitors of HIV-1. *J. Med. Chem.* **2001**, *44* (12), 1866−1882.
(41) Chan, J. Unpublished data.
(42) Hazen, R. J.; Harvey, R. J.; St Clair, M. H.; Ferris, R. G.; Freeman, G. A.; Tidwell, J. H.; Schaller, L. T.; Cowan, J. R.; Short, S. A.; Romines, K. R.; Chan, J. H.; Boone, L. R. Anti-human immunodeficiency virus type 1 activity of the nonnucleoside reverse transcriptase inhibitor GW678248 in combination with other antiretrovirals against clinical isolate viruses and in vitro selection for resistance. *Antimicrob. Agents Chemother.* **2005**, *49* (11), 4465−4473.
(43) Petropoulos, C. J.; Parkin, N. T.; Limoli, K. L.; Lie, Y. S.; Wrin, T.; Huang, W.; Tian, H.; Smith, D.; Winslow, G. A.; Capon, D. J.; Whitcomb, J. M. A novel phenotypic drug susceptibility assay for human immunodeficiency virus type 1. *Antimicrob. Agents Chemother.* **2000**, *44* (4), 920−928.
(44) Yang, S. S.; Pattabiraman, N.; Gussio, R.; Pallansch, L.; Buckheit, R. W.; Bader, J. P. Cross-resistance analysis and molecular modeling of nonnucleoside reverse transcriptase inhibitors targeting drug-resistance mutations in the reverse transcriptase of human immunodeficiency virus. *Leukemia* **1997**, *11*, 89−92.

JM061117M